Materials Today Communications 26 (2021) 101897

Contents lists available at ScienceDirect

Materials Today Communications

journal homepage: www.elsevier.com/locate/mtcomm

Machine learning-aided design of aluminum alloys with high performance

Umer Masood Chaudry [a], Kotiba Hamad [a,*], Tamer Abuhmed [b,*]

[a] School of Advanced Materials Science & Engineering, Sungkyunkwan University, Suwon 16419, South Korea
[b] College of Computing, Sungkyunkwan University, Suwon 16419, South Korea

ARTICLE INFO

Keywords:
Aluminum alloys
Machine learning
Hardness
Age hardening
Gradient boosted tree

ABSTRACT

In this work, various machine learning (ML) techniques were employed to accelerate the designing of aluminum (Al) alloys with improved performance based on the age hardening concept. For this purpose, data of Al-Cu-Mg-*x* (*x*: Zn, Zr, etc.) alloys, including composition, aging condition (time and temperature), important physical and chemical properties, and hardness were collected from the literature to train the ML algorithms for predicting Al alloys with superior hardness. The results showed that the model obtained by the gradient boosted tree (GBT) could efficiently predict the hardness of unexplored alloys.

1. Introduction

Recently, lightweight metals such as aluminum (Al) and magnesium (Mg), have been receiving great attention for structural applications [1–7]. These materials have significant impacts on power consumption and accordingly can reduce the need for fossil fuels. In particular, Al alloys are precipitation-hardened (age-hardened), with high wear resistance, high specific strength, and outstanding formability [8–12]. The main issue in this kind of alloys that the age-hardening method is a complicated, costly, and time-consuming process based on the trial and error approach to identify useful material composition and optimum conditions (temperature and time) for desired properties. To avoid fabrication-experimentation cycles that are time-consuming and expensive, an effective and efficient method is required which can generate, manage, and utilize the available data to significantly expedite the discovery of new materials. We propose the use of machine learning (ML) approaches to predict the properties of specific material combinations based on previous data available from the literature. ML was successfully exploited in functional and advanced materials to explore new material combinations with desired properties [13–17]. For instance, Xue et al. employed the ML model to predict the martensitic transformation temperature of shape memory alloy (SMA) and proposed a Landau-type model for understanding the mechanisms that control the transformation temperature of NiTi-based SMAs [16]. Moreover, the experimental work successfully validated the model, where the transformation temperature of 182.89 °C was measured for $Ti_{50}Ni_{25}Pd_{25}$ in comparison to the 189.56 °C as predicted by ML model. Building an accurate ML model that predicts the desired material properties is crucially depends on the accuracy of the underline data used to train the ML algorithm. Therefore, the datasets of the previous fabricated experiments must have enough uniformity and accuracy. Although ML schemes have already beginning to make major inroads within materials science, yet a little number of studies have been conducted to predict the mechanical properties of materials [18,19]. Shen et al. developed a ML model guided by the physical metallurgy (PM) parameters (equilibrium volume fraction of precipitates, driving force per precipitation) to design ultrahigh strength stainless steel [18]. The PM-guided ML model successfully predicted the required composition, where an excellent agreement between the predicted and experimental mechanical properties of fabricated prototype alloy was achieved. Moreover, it was also demonstrated that the utilization of the PM parameters significantly enhanced the efficiency and accuracy of the ML model. Very recently, Mohamadreza et al. used ML to correlate the material properties and to predict the crystallographic orientations of Mg alloy using mechanical testing values as an input data set [19]. The results revealed that ML successfully predicted the pole figures for various conditions without knowing the dependencies of physical variables. Hence, it can be concluded that the ML framework can be used to avoid the hit and trial time-consuming cycles and to successfully expedite the material discovery by correlating the interdependencies of various features and targeted property. In this study, accordingly, several ML models have been employed to accelerate the designing of Al alloys with improved performance. Here, due to its importance in various structural applications, Al-Cu-Mg-*x* alloy was selected as the base material in the present work.

* Corresponding authors.
E-mail addresses: hamad82@skku.edu (K. Hamad), tamer@skku.edu (T. Abuhmed).

https://doi.org/10.1016/j.mtcomm.2020.101897
Received 21 October 2020; Received in revised form 16 November 2020; Accepted 16 November 2020
Available online 20 November 2020

2. Procedure

In this study, features, including composition and aging conditions (temperature and time), and the related property (hardness) of various Al-Cu-Mg-*x* based alloys were collected from previous works (1592 cases), and those are arranged and presented in the supplementary material. It is well-known that composition and aging conditions are the most straightforward parameters that control the characteristics of precipitates (volume fraction, morphology, and their relation to the matrix) and the associated properties in age-hardened Al alloys [20–23]. To represent the composition in the employed ML algorithm besides processing conditions (temperature and time), physical properties and electronic structure parameters (15 features) of each constitute were employed using the weighted fraction concept as follow:

$$X = \sum C_i X_i \tag{1}$$

where X is the weighted fraction of the feature, X_i is the feature (electronegativity, atomic number, atomic mass, atomic radius, valance electrons, boiling point, specific heat, melting point, heat of vaporization, heat of fusion, group, period, electro-affinity, density, thermal conductivity) of the element i and C_i the concentration of the element i in the alloy. The features used in the previous equation (physical properties and electronic structure) were obtained from [24]. The collected data (hardness, processing conditions, and compositions) shown the supplementary material went through an outlier detection algorithm called Local Outlier Factor (LOF) [25] which is based on the local density deviation of a given data point, i.e., condition with respect to K = 10 neighbors. The LOF eliminated all outlier conditions before we randomly separated our collected dataset into two sets, training dataset (900 conditions) and testing dataset (600 conditions). The former set of data was used to train and learn the model using six different algorithms, including general linear model (GLM), deep learning (DL), decision tree (DT), random forest (RF), gradient boosted tree (GBT) and support vector machine (SVM). The latter, in turn, was used to examine the reliability of the trained models reached by the six algorithms. The performance of the employed algorithms will be compared using mean squared error (MSE) and R^2 statistics for each model [18]. The MSE determines the variations between the model-predicted value, (y_i) and measured value ($\hat{y}_i$), and this can be given as follow:

$$MSE = \frac{1}{n}\sum_{i=1}^{n}(y_i - \hat{y}_i)^2 \tag{2}$$

According to the MSE values, that predication is more accurate in the algorithm which leads to a smaller MSE. The R^2 can also be used to expect the prediction accuracy of the used algorithm (the closer R^2 to 1 the more accurate predictions), where R^2 is calculated as follow:

$$R^2 = 1 - \frac{\sum_{i=1}^{n}(y_i - \hat{y}_i)}{\sum_{i=1}^{n}(y_i - \bar{y}_i)} \tag{3}$$

where $\bar{y}_i$ is the mean value of the y_i

3. Results and discussion

To design an accurate ML model, the selection of appropriate features that are directly associated with the targeted property is inevitable. Usually, using many features that are poorly related with the desired property, can result in complexity of the model and hence, eliminating those features can result in a simpler and understandable model. Accordingly, in the present work, following the creation of the training and testing datasets, two main feature selection techniques called filter and wrapper were applied to select the best features that should be included in the final ML model. The filter technique is based on features Pearson correlation (PC) to filter out the least promising features (Fig. 1a). Based on the PC coefficient (r) which has values between −1 to +1, one can determine whether two variables are linearly correlated (positive or negative correlations) (r = ±1) or they are poorly correlated (r→0). In the first case, where the two variables are correlated, one of them is enough to be used as a predictor in the built model, however, in

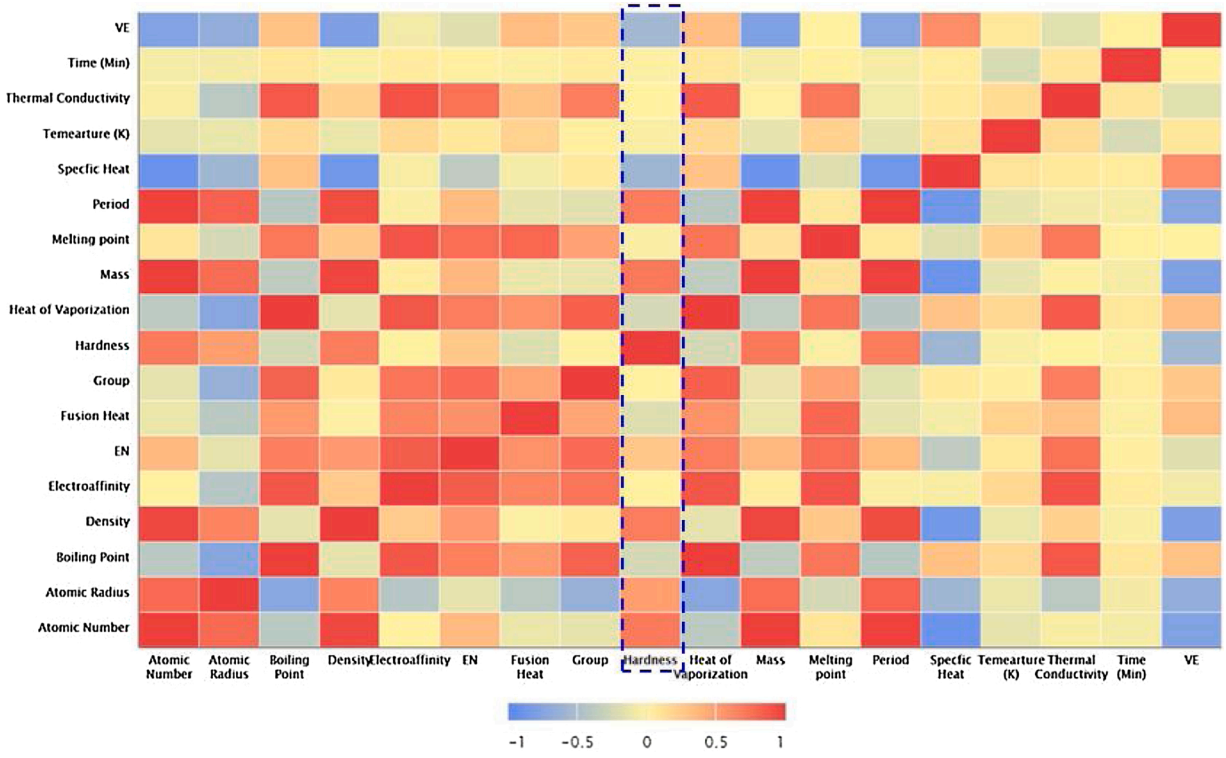

Fig. 1. (a) Pearson correlation matrix of all features used in the present work. The features with correlation coefficient (r) between -0.45 and +0.45 were considered to be uncorrelated.

the second, both the two uncorrelated variables should be included in the model to describe the behavior. In addition to the r value, the relevant color also corresponds to the correlation between various features, where the darker the color the more significant is the correlation between the features. Accordingly and using Fig. 1, four features-namely; atomic number, mass, density, and period- can be excluded during training and testing the model. Here, r values between −0.45 to +0.45 were taken to determine uncorrelated variables. More filtration was also applied using the Wrapper feature selection (WFS) technique, where the importance of a feature subset based on training and testing of a subset on the regression algorithm is measured. Accordingly, the features subset with the best regression results is chosen to be included later on during the training and testing of the full dataset. Based on this procedure, three additional features, electron affinity, thermal conductivity, and group were excluded from the training and testing dataset. On the other hand, the important features that might be promising for building the predictive model were found to be: aging time, aging temperature, electronegativity, atomic radius, valence electrons, boiling point, specific heat, melting point, heat of vaporization, heat of fusion. From the material science point of view, those are also important when considering the aging behavior of various Al alloys. For example, intermetallic compounds formed during solidification and aging treatment of the investigated alloy, and the structure of these compounds are highly influenced by the electronegativity difference among the constituent elements in the alloy. In addition, aging time and temperature are of importance to control the morphology of the evolved intermetallic compounds (precipitate shape and size) and their distribution in the matrix (uniform or non-uniform) during the aging heat treatment of the alloy. This leads to say that the feature selection results reached in the present ML work are, somehow, consistent with the materials science concepts.

Fig. 2a shows the validation process performed by 600 conditions on the trained models obtained by the six algorithms used in the present work. It is clearly seen that all models, except GLM and DL, exhibit reasonable reliability at lower values of hardness (lower than 150 Hv), whereas less accuracy was noted for all models at the higher values (>150 Hv). Such behavior is mainly related to the experience got by the various models during the training of this data (900 conditions). Based on the hardness distribution profile of this data shown in Fig. 2b, one can notice that the hardness is mainly distributed in the range of low values (<150 Hv), and accordingly, the various models were less trained on the high values of hardness as compared to the low values. To compare the performance, $R^{2,}$ and MSE values of these models were presented in Fig. 2c. The results of R^2 and MSE confirmed that the trained model reached by the SVM was the most accurate to predict the hardness using the features of the testing dataset, where 0.84 and 12.79 values of R^2 and MSE were obtained for SVM, respectively. On the other hand, although the SVM showed the higher capability to predict the hardness values as compared to other algorithms, the accuracy of the SVM model still less as compared to those reported in previous work [18]. In this regard, to improve the performance of various models, and thus, to enhance their hardness-predictability in the present work, a so-called hyperparameter optimization is needed. Using the training and testing data, we optimized the ML models and get the final hyperparameters as listed in Table 1. Fig. 2d and e show the experimental hardness and the hardness predicted by the optimized models for the test dataset and a comparison between different models (non-optimized and optimized) in terms of R^2 and MSE. It is clearly seen that all models, except that of GLM and DL, exhibited high prediction performance after the optimization, where R^2 values of 0.9, 0.95, 0.94, and 0.93 were obtained for DT, RF, GBT, and

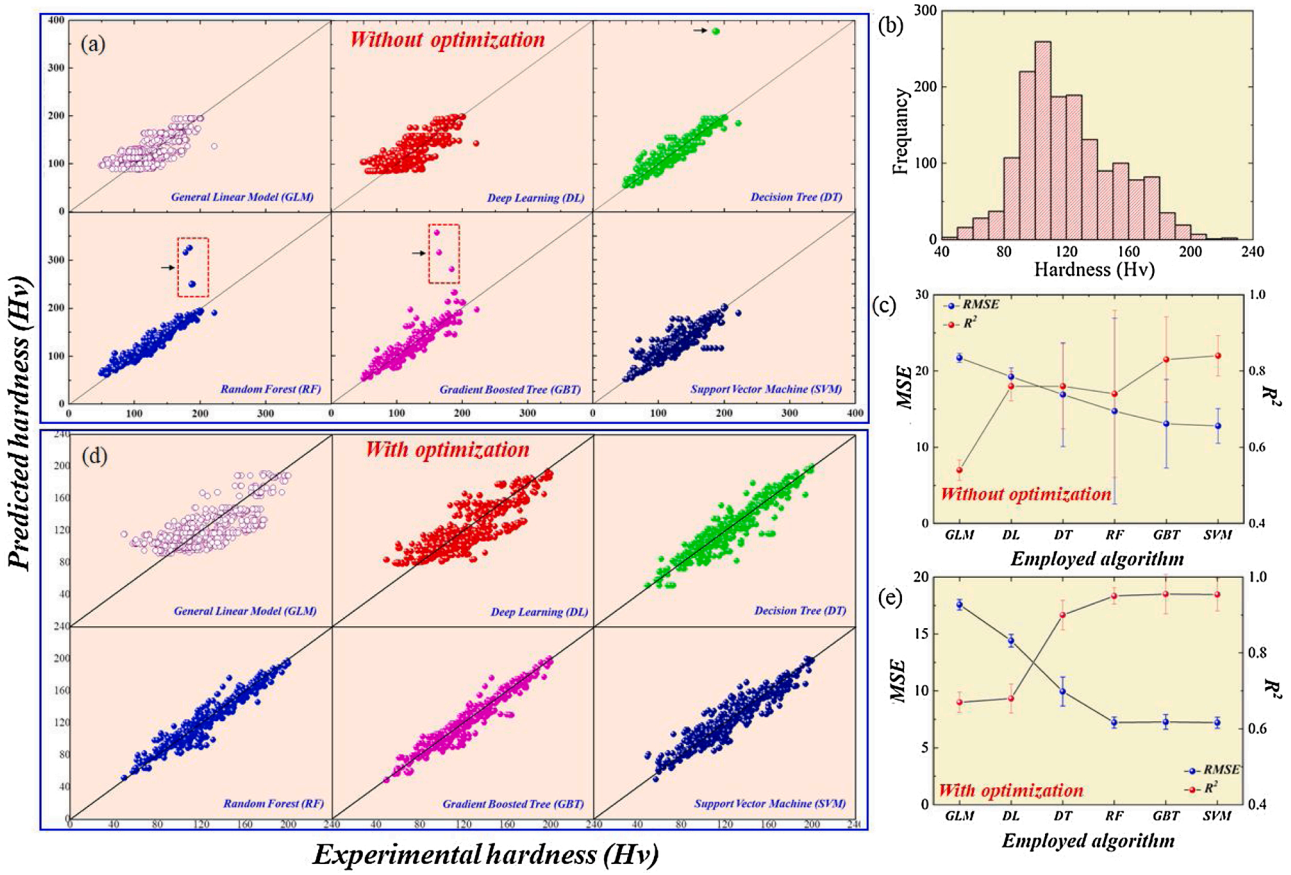

Fig. 2. (a,c) and (d,e) Experimental vs predicted hardness of various models of the testing data set and the related R^2 and MSE recorded for the employed algorithms without optimization and with optimization, respectively, (b) Hardness distribution profile for the input dataset.

Table 1
Best experimental hyperparameters of all the ML algorithms trained on the dataset used in the present work.

Algorithm	Experiment Hyperparameter
GM	Alpha = 0.5, Lambda = 0.0762, kernel = Gaussian
DL	Layers = 3, Layer size = 50, Activation = Rectifier, Learning rate = 0.001, L1 = 1.0E-5, Epochs = 10
DT	Criterion = Gini, max depth = 5, minimum leaf split = 2
RF	Criterion = gain ratio, Max depth = 15, number of trees = 70, Minimum leaf split = 2
GBT	Criterion = gain ratio, Max depth = 7, number of trees = 150, Learning rate = 0.01
SVM	Support Vectors = 926, Cost = 100, Solver – lbfgs, Gamma = 1, Learning rate = adaptive

SVM, respectively. In addition, it is worth noting the optimization process had a negative effect on the predictability of the DL model, and this is caused by the need for a large data space for training such kind of models (DL). Furthermore, the GBT model not only is the best based on the R^2 (~0.94) but also is well-predictive in the whole hardness range. The GBT model is an ensemble model of multiple DT regressors. The main strength of the GBT model resides in creating a strong prediction model using multiple weak regression trees. Trees are constructed greedily during the training, and all the trees are used to predict a new value at the testing time. To ensure the quality of the GBT predicted values, a regularization should be applied to the GBT model to improve the performance and prevent the model from overfitting to the training data. Accordingly, the GBT-based model will be used in the adaptive design of the alloy with improved performance. For this purpose, a virtual space of features was generated based on the composition and processing parameters (aging time and temperature), where ~500 K cases were included in this space. The counterpart hardness of the features in this space was then predicted using the optimized GBT model. Fig. 3 shows the hardness distribution as predicted for the virtual space using the optimized GBT model, where values higher than 185 Hv were just considered here. It can be seen from Fig. 3 that a large number of conditions (~3500) are predicted to show improved hardness (>185 Hv). Using this insight, some compositionally lean alloys were selected as promising Al-based materials to be considered from further experimental investigations with the corresponding aging conditions (Aging temperature and time) are listed in Table 2. A wide range of aging temperature (300−500 K) and aging time (0–7000 min s) were used to predict the hardness of Al alloys and only those with the optimum hardness values are presented in Table 2. For example, the Al alloy that contains 3 wt.% Cu, 3 wt.% Mg and 3.5 wt.% Sn is expected to have a hardness value of 195 when aging at 100 °C for 2000 min. Very recently, Shuai et al. has reported the significant influence of Sn on the hardening

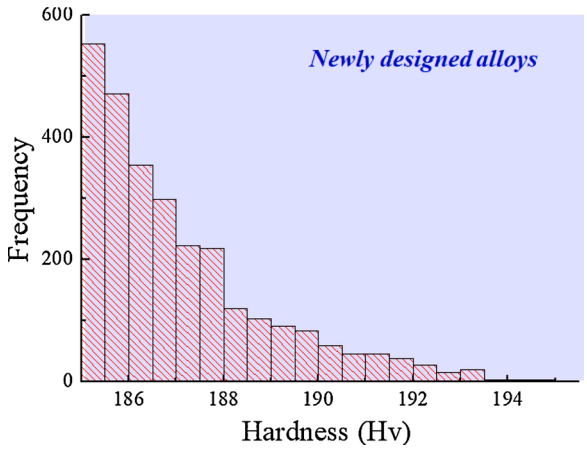

Fig. 3. The hardness data of the newly designed alloys as predicated by the GBT-based model.

behavior of the Al-Cu-Mg alloy [25]. The results revealed that the alloying of Al-Cu-Mg with Sn can lead to the formation of Mg_2Sn particles in the as-quenched alloy, and these particles, in turn, were found to contribute to the formation of θ' phase precipitates (Al_2Cu) during the aging. As a result, Sn addition to Al-Cu-Mg alloy facilitated the particle-simulated nucleation (PSN) effect and enhanced the grain boundary pinning effect due to increased precipitation behavior resulting in high strength.

To determine the accuracy of the predictive model reached in the present work, the aging behavior of an alloy in the predicted compositions was compared to that of a similar composition reported very recently (Al-4Cu-0.5Mg-0.15Si-0.1Sc) [26]. For predicting the aging curves of this alloy, the related features were collected based on the elements characteristics (electronegativity, atomic radius, valence electrons, etc.) and processing conditions (aging temperature and time). The collected features were employed in the GBT-based model built in the present work to estimate the hardness values, and then, to compare them with the experimental counterparts. Fig. 4a presents the experimental and predicted aging curves for Al-4Cu-0.5Mg-0.15Si-0.1Sc (wt. %) alloy aged at 175 °C and 225 °C for a wide range of time. As it is evident from Fig. 4a, the model successfully predicted the aging behavior of the alloy with reliable accuracy for both the aging temperatures (175 °C and 225 °C). The microstructure evolution and the precipitation during the heat treatment were used to figure out the aging behavior observed in the this alloy. The transition electron microscopy (TEM) micrograph presented in Fig. 4b shows the various type of precipitates that formed during the aging of this alloy. Mainly, two types of precipitates were observable in the sample treated at 175 °C for 930 h, those are plate-like θ' phase (Al_2Cu) and cubic σ phase ($Al_5Cu_6Mg_2$), as indicted by arrows in Fig. 4b. The θ' phase was distributed homogenously throughout the structure with fine size (3 nm thickness and 50 nm diameter), and this was additionally confirmed through the energy dispersive spectroscopy (EDS) maps taken from the samples heat-treated at 225 °C for 930 h, as shown in Fig. 4c. The uniform distribution of such fine plates leads usually to the improved performance of this Al alloy. Hence, it can be concluded that the designed model can be efficient to predict the aging behavior of any Al alloys at a certain temperature with adequate accuracy. Accordingly, the developed model can be utilized for predicting the properties of yet to be synthesized alloying combinations which, in turn, can accelerate the discovery of suitable alloys with optimum properties.

The design problem presented in this work was addressed by setting the goal of predicting the composition and aging conditions (temperature and time) that would be needed to fabricate high-performance Al-Cu-Mg-*x* alloys, and the strategy used for this purpose is shown in Fig. 5. Initially, the dataset for training the ML algorithm and for building the predictive model was collected from the papers reported on the aging behavior of Al-Cu-Mg-*x* alloys. Before training the ML algorithms, the dataset was processed in order to remove the outliers and unnecessary features. Later on, the processed data was divided into a training set, that is used for the learning process, and a testing set to evaluate the built model and to select the best ML algorithm based on the R^2 and MSE values. The best model was used to predict the hardness of a virtual dataset containing new compositions and various aging conditions. Based on the predicted results accuracy, we found that the proposed framework can be extremely useful for accelerating the search for Al alloy compositions and related aging conditions. Accordingly, this work has demonstrated the power of ML models as a promising tool to fabricate high-performance materials. It is pertinent to mention that the prediction capability of ML models is strongly dependent on the size and quality of the input dataset in addition to the diversity and distribution of the input features that can comprehensively describe the underneath mechanisms.

In recent years, the excellent development of various physical modeling techniques and computationally-aided design strategies by utilizing integrated computational materials engineering (ICME) has

Table 2
Maximum hardness values of some compositions with the corresponding aging conditions (aging temperature and time) as predicted by the GBT-based model.

Al	Cu	Mg	Si	Zn	Zr	Mn	Ag	Fe	Sn	Cr	Ge	Temperature (K)	Time (min)	Hardness
0.905	0.03	0.03	0	0	0	0	0	0	0.035	0	0	373	2000	**195.25**
0.915	0.04	0.01	0.02	0.015	0	0	0	0	0	0	0	475	700	**194.8602**
0.92	0.04	0.01	0.02	0	0	0.01	0	0	0	0	0	475	700	**193.8269**
0.925	0.04	0.015	0.005	0	0	0	0	0	0	0	0.015	475	700	**193.5077**
0.915	0.04	0.015	0.01	0	0	0	0	0	0	0	0.02	475	700	**193.4039**
0.915	0.04	0.015	0.02	0	0	0	0	0	0.01	0	0	475	700	**193.3844**
0.925	0.04	0.015	0	0	0	0	0	0	0	0	0.02	475	700	**193.3744**
0.935	0.04	0.01	0	0	0	0	0	0	0	0	0.015	475	700	**193.3628**
0.915	0.04	0.015	0.015	0	0	0	0	0	0	0	0.015	475	700	**193.3273**
0.925	0.04	0.015	0.01	0	0	0	0	0	0.01	0	0	475	700	**192.801**
0.895	0.04	0.02	0.02	0	0	0	0	0	0	0	0.025	475	700	**192.7703**
0.925	0.04	0.01	0.015	0	0	0.01	0	0	0	0	0	475	700	**192.2091**
0.91	0.04	0.02	0.02	0	0	0	0.01	0	0	0	0	475	900	**191.6235**
0.92	0.04	0.015	0.02	0	0	0	0.005	0	0	0	0	475	700	**191.6132**
0.935	0.04	0.01	0.01	0	0	0	0.005	0	0	0	0	475	700	**191.475**
0.915	0.04	0.015	0.015	0	0	0	0	0	0	0.015	0	475	700	**191.2946**
0.905	0.04	0.02	0.02	0	0	0	0	0.015	0	0	0	475	700	**191.0571**
0.91	0.04	0.01	0.015	0	0.025	0	0	0	0	0	0	400	3000	**187.923**

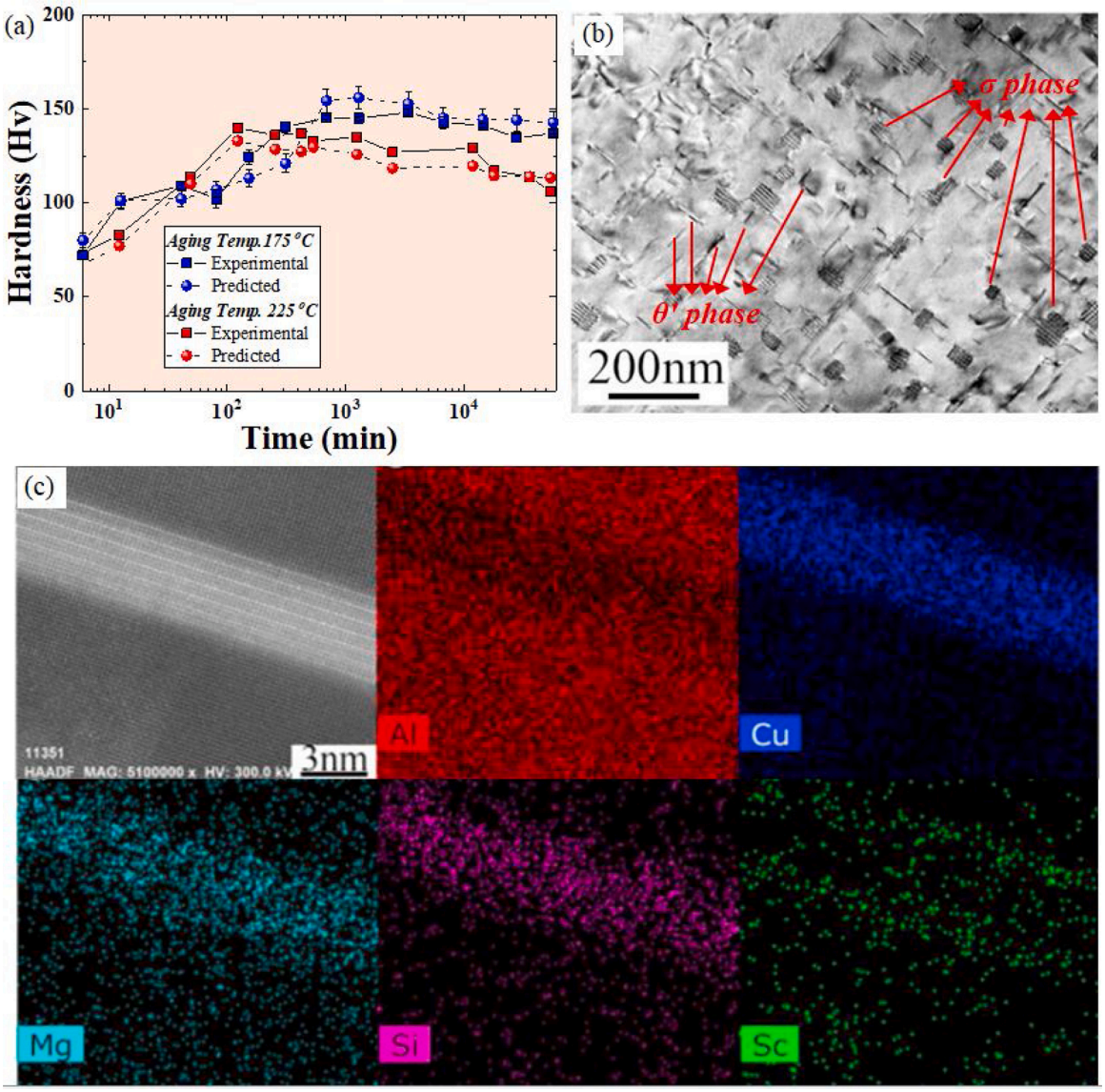

Fig. 4. (a) Experimental and predicted isothermal aging curves of Al-4Cu-0.5Mg-0.15Si-0.1Sc alloy at 175 and 225 °C. (b) TEM micrographs of Al-4Cu-0.5Mg-0.15Si-0.1Sc alloy aged at 175 °C for 930 h showing the evolution of plate-like θ' phase and cubic σ phase [26]. (c) High-angle annular dark-field scanning transmission electron microscopy (HAADF-STEM) and the related EDS maps of the alloy heat-treated at 225 °C for 930 h, confirming the formation of the plate-like θ' phase [26].

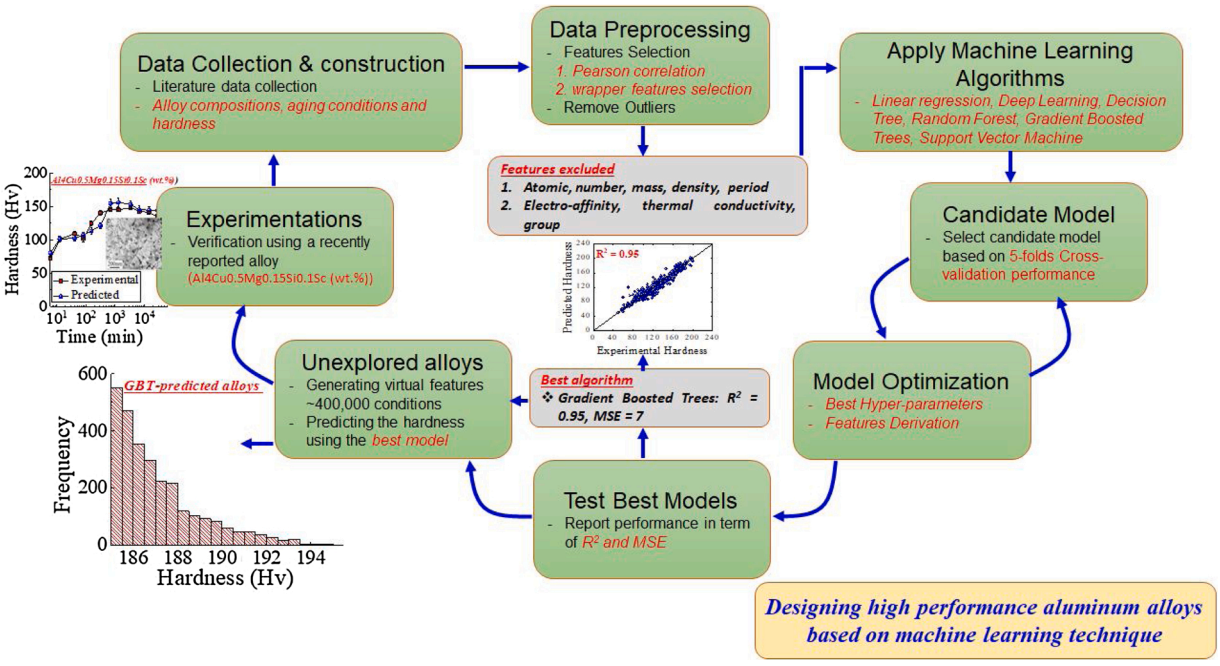

Fig. 5. The loop used for designing high performance Al-Cu-Mg alloys based on the machine learning technique.

helped to unveil the overall underlaying mechanisms in a typical condition. Hence, considering the underlying microstructural characteristics and using suitable descriptors for representing the overall undergoing mechanisms can be the benchmark for systematic prediction with significant reliability. In the current work, for instance, the prediction has been solely made by exploiting the compositional and processing features and hence, the overall prediction accuracy of ML models can be significantly enhanced by incorporating more internal parameters (the strengthening mechanisms involved and the characteristics of formed precipitates) in addition to the external parameters (composition and processing conditions). The ML cannot only make the predictions based on the statistically learn trends but can also help in understating the mechanism and metallurgical aspects related to the age hardening of Al alloys. Such a relationship between the external features (composition and processing conditions) and internal parameters (precipitate-related features) can be made through thermodynamic calculations using various software such as Thermo-Calc® [27] and Calphad® [28]. Up to this end, our expectation towards future works on the ML-guided the designing of high performance Al alloys will be to employ the same ML procedures used in the present work, and to utilize the internal-structural-features which are related to the characteristics of evolved precipitates (type, volume fraction, shape and size). Additionally, since the ensemble model of GBT achieved the best prediction in the present work, the application of alternative ensemble regressors and their impacts on the prediction of high performance Al alloys can be also considered in future works.

4. Conclusions

In the present work, ML models were used to identify the promising Al alloys with superior hardness. The physical and chemical features, compositions, and age hardening conditions (time, temperature) were collected from the literature for training and testing the various ML models. The ML models were implemented to develop a correlation between the input data and to predict the hardness of promising Al alloys under various age-hardening conditions. The results revealed that the GBT model was best amongst others with R^2 and MSE of 0.94 and 7.27, respectively. Finally, the date from the recently published literature also proved the prediction accuracy of the constructed model. Hence, the designed ML model can be successfully employed to identify the high performance of Al alloys by avoiding the time-intensive hit and trial experimentation.

Data availability

The data used in the current study can be downloaded from the supplementary information.

Declaration of Competing Interest

Authors have no conflict of interest.

Acknowledgments

This research was supported by National Research Foundation (NRF) of South Korea (2020R1A2C1004720).

Appendix A. Supplementary data

Supplementary material related to this article can be found, in the online version, at doi:https://doi.org/10.1016/j.mtcomm.2020.101897.

References

[1] J. Hirsch, Recent development in aluminium for automotive applications, Trans. Nonferrous Met. Soc. China 24 (2014) 1995–2002.
[2] E.A. Starke Jr., J.T. Staley, Application of modern aluminum alloys to aircraft, Prog. Aerosp. Sci. 32 (1996) 131–172.
[3] N. Kashaev, V. Ventzke, G. Çam, Prospects of laser beam welding and friction stir welding processes for aluminum airframe structural applications, J. Manuf. Process. 36 (2018) 571–600.
[4] T. Dursun, C. Soutis, Recent developments in advanced aircraft aluminium alloys, Mater. Des. 56 (1980–2015) (2014) 862–871.
[5] U.M. Chaudry, K. Hamad, J.-G. Kim, On the ductility of magnesium based materials: a mini review, J. Alloys. Compd. 792 (2019), 652e64.
[6] N. Kim, Critical Assessment 6: magnesium sheet alloys: viable alternatives to steels? Mater. Sci. Technol. 30 (2014) 1925–1928.
[7] B. Mordike, T. Ebert, Magnesium: properties—applications—potential, Mater. Sci. Eng. A 302 (2001) 37–45.

[8] S. Liang, S. Wen, J. Xu, X. Wu, K. Gao, H. Huang, et al., The influence of Sc–Si clusters on aging hardening behavior of dilute Al-Sc-(Zr)-(Si) alloy, J. Alloys. Compd. (2020), 155826.
[9] W. Yang, W. Shen, R. Zhang, K. Cao, J. Zhang, L. Liu, Enhanced age-hardening by synergistic strengthening from Mg-Si and Mg-Zn precipitates in Al-Mg-Si alloy with Zn addition, Mater. Charact. (2020), 110579.
[10] W. Tu, J. Tang, Y. Zhang, L. Cao, L. Ma, Q. Zhu, et al., Influence of Sn on the precipitation and hardening response of natural aged Al-0.4 Mg-1.0 Si alloy artificial aged at different temperatures, Mater. Sci. Eng. A 765 (2019), 138250.
[11] L. Wu, Y. Li, X. Li, N. Ma, H. Wang, Interactions between cadmium and multiple precipitates in an Al-Li-Cu alloy: improving aging kinetics and precipitation hardening, J. Mater. Sci. Technol. 46 (2020) 44–49.
[12] K. Yamamoto, M. Takahashi, Y. Kamikubo, Y. Sugiura, S. Iwasawa, T. Nakata, et al., Effect of Mg content on age-hardening response, tensile properties, and microstructures of a T5-treated thixo-cast hypoeutectic Al–Si alloy, Mater. Sci. Eng. A (2020), 140089.
[13] Y. Liu, B. Guo, X. Zou, Y. Li, S. Shi, Machine learning assisted materials design and discovery for rechargeable batteries, Energy Storage Mater. (2020).
[14] B. Roter, S. Dordevic, Predicting new superconductors and their critical temperatures using machine learning, Physica C: Supercond. Appl. (2020), 1353689.
[15] A.D. Orme, I. Chelladurai, T.M. Rampton, D.T. Fullwood, A. Khosravani, M. P. Miles, et al., Insights into twinning in Mg AZ31: a combined EBSD and machine learning study, Comput. Mater. Sci. 124 (2016) 353–363.
[16] D. Xue, D. Xue, R. Yuan, Y. Zhou, P.V. Balachandran, X. Ding, et al., An informatics approach to transformation temperatures of NiTi-based shape memory alloys, Acta Mater. 125 (2017) 532–541.
[17] Z. Pei, J. Yin, Machine learning as a contributor to physics: understanding Mg alloys, Mater. Des. 172 (2019), 107759.
[18] C. Shen, C. Wang, X. Wei, Y. Li, S. van der Zwaag, W. Xu, Physical metallurgy-guided machine learning and artificial intelligent design of ultrahigh-strength stainless steel, Acta Mater. 179 (2019) 201–214.
[19] M. Shariati, W.E. Weber, J. Bohlen, G. Kurz, D. Letzig, D. Höche, Enabling intelligent Mg-sheet processing utilizing efficient machine-learning algorithm, Mater. Sci. Eng. A (2020), 139846.
[20] S. Jin, T. Ngai, L. Li, Y. Lai, Z. Chen, A. Wang, Influence of natural aging and pre-treatment on the precipitation and age-hardening behavior of Al-1.0 Mg-0.65 Si-0.24 Cu alloy, J. Alloys. Compd. 742 (2018) 852–859.
[21] N.D. Alexopoulos, Z. Velonaki, C.I. Stergiou, S.K. Kourkoulis, Effect of ageing on precipitation kinetics, tensile and work hardening behavior of Al-Cu-Mg (2024) alloy, Mater. Sci. Eng. A 700 (2017) 457–467.
[22] F. Qian, E.A. Mørtsell, C.D. Marioara, S.J. Andersen, Y. Li, Improving ageing kinetics and precipitation hardening in an Al-Mg-Si alloy by minor Cd addition, Materialia 4 (2018) 33–37.
[23] Y. Weng, Z. Jia, L. Ding, Y. Pan, Y. Liu, Q. Liu, Effect of Ag and Cu additions on natural aging and precipitation hardening behavior in Al-Mg-Si alloys, J. Alloys. Compd. 695 (2017) 2444–2452.
[24] http://periodictable.com.
[25] S. Dai, Z. Bian, W. Wu, J. Tao, L. Cai, M. Wang, et al., The role of Sn element on the deformation mechanism and precipitation behavior of the Al–Cu–Mg alloy, Mater. Sci. Eng. A 792 (2020), 139838.
[26] S. Liang, S. Wen, X. Wu, H. Huang, K. Gao, Z. Nie, The synergetic effect of Si and Sc on the thermal stability of the precipitates in AlCuMg alloy, Mater. Sci. Eng. A (2020), 139319.
[27] http://www.thermocalc.com. Thermo-calc Software.
[28] L. Kaufman, H. Bernstein, Computer Calculation of Phase Diagrams. With Special Reference to Refractory Metals, 1970.